NJC

Accepted Manuscript

This is an *Accepted Manuscript*, which has been through the Royal Society of Chemistry peer review process and has been accepted for publication.

Accepted Manuscripts are published online shortly after acceptance, before technical editing, formatting and proof reading. Using this free service, authors can make their results available to the community, in citable form, before we publish the edited article. We will replace this *Accepted Manuscript* with the edited and formatted *Advance Article* as soon as it is available.

You can find more information about *Accepted Manuscripts* in the Information for Authors.

Please note that technical editing may introduce minor changes to the text and/or graphics, which may alter content. The journal's standard Terms & Conditions and the Ethical guidelines still apply. In no event shall the Royal Society of Chemistry be held responsible for any errors or omissions in this *Accepted Manuscript* or any consequences arising from the use of any information it contains.

ROYAL SOCIETY OF CHEMISTRY

www.rsc.org/njc

Sol-gel chemistry for graphene-silica nanocomposite films

Plinio Innocenzi[1], Luca Malfatti[1], Barbara Lasio[1], Alessandra Pinna[1], Danilo Loche[2], Maria F. Casula[2], Valeria Alzari[3], Alberto Mariani[3]

[1]Laboratorio di Scienza dei Materiali e Nanotecnologie, CR-INSTM, Università di Sassari, Palazzo Pou Salid, Piazza Duomo 6, 07041 Alghero (SS), Italy

[2] Dipartimento di Scienze Chimiche e Geologiche Università di Cagliari, 09042 Monserrato, (CA) (Italy)

[3]Dipartimento di Chimica e Farmacia, Università di Sassari, Local INSTM Unit, Via Vienna 2, 07100 Sassari, Italy

Abstract

Fabrication of graphene nanocomposite films via sol-gel chemistry is still a challenging task because of the low solubility of graphene in common solvents. In the present work we have successfully developed a suitable synthesis employing a solution of exfoliated graphene in 1-vinyl-2-pyrrolidone that is added to an anhydrous sol of silicon tetrachloride in ethanol. Thin graphene-silica films with high optical transparency have been obtained; the graphene sheets are composed of two layers and do not aggregate after incorporation in the matrix upon a large range of concentrations. Thermal processing of the silica films allows a full removal of 1-vinyl-2-pyrrolidone without oxidation or degradation of the graphene sheets which are embedded in the oxide.

Introduction

The linear and nonlinear optical properties of graphene have recently attracted much attention;[1] dispersions of graphene single sheets have shown giant broadband nonlinear optical absorption response[2,3] and optical limiting properties[4]. The broadband response of graphene from the visible to the near infrared range, in particular, represents an intrinsic advantage in comparison to C_{60} which exhibits a nonlinear optical response with reverse saturable absorption only in the visible region[5].

Development of graphene-based nonlinear optical devices, such as optical limiters, requires the preparation of optically transparent films with controlled thickness and graphene concentration. To avoid laser damage of the system, graphene should be incorporated in oxide or organic-inorganic matrixes because it exhibits a higher damage threshold with respect to organic polymers.

Sol-gel chemistry is the most suitable route for preparing nanocomposites films from a liquid phase; an intrinsic advantage of the method is the low temperature material synthesis which allows incorporating organic molecules into the matrix avoiding degradation due to high temperature processing. This route has been successfully applied to incorporate fullerene derivatives into hybrid sol-gel films; the material has shown excellent optical limiting properties and good resistance to laser damage.[5,6] Design of the proper synthesis for films and bulk materials via sol-gel is, however, not a simple goal, because uncontrolled aggregation is a common side effect observed in the precursor sol.[7]

Some examples of graphene-based nanocomposite[8] films have been already reported; most of these examples regards graphene-titania nanocomposites which have been prepared with the purpose of exploiting the photocatalytic properties of graphene. Graphene has been incorporated into mesoporous titania[9] and silica[10], titania[11] and other nanocomposites[12] using different strategies; while these studies have been devoted to the development of applications, a fundamental understanding of the synthesis has still to be performed. In the present work, we have done a basic study of a graphene-silica

sol-gel system with the purpose of obtaining transparent nanocomposites for optical applications.

Experimental

1-Vinyl-2-pyrrolidone (NVP, Sigma-Aldrich), graphite (Sigma-Aldrich), silicon tetrachloride ($SiCl_4$ 99.9%, Sigma-Aldrich), absolute ethanol (EtOH, 99.8% Fluka) were used as received without further purification. P-type/boron doped, (100) oriented, 400 μm thick silicon wafers (Si-Mat) and 1.2 mm thick silica slides (Heraeus, UV grade) were used as substrates.

Preparation of exfoliated graphene dispersion.

The graphene dispersion was prepared starting from a NVP solution (50 ml) containing 5 wt % of graphite flakes. The solution was placed into a tubular plastic reactor (inner diameter 15 mm) and sonicated for 24 h at 25°C (Ultrasound bath EMMEGI, 0.55 kW). The dispersion was centrifuged for 30 min at 4000 rpm to precipitate the remaining graphite flakes and the gray/black supernatant liquid was recovered. 25 ml of the liquid was then used to determine the graphene concentration; the liquid was filtered through polyvinylidene fluoride filters (pore size 0.22 μm) to directly weigh the amount of dispersed graphene. By using this method, a concentration of 2.27 mg ml^{-1} was obtained.

Sol preparation.

Silica precursor sol was obtained by mixing 3 ml of silicon tetrachloride with 45.78 ml of ethanol with a molar ratio of 1 : 30. The graphene dispersions (43.7, 87.5, 175, 350 and 700 μl) were mixed with the silica sol (7 ml) and then sonicated for 30 minutes before film deposition. The syntheses were done at relative humidity (RH) of 25% and the solutions of precursors have been poured in sealed bottles immediately after mixing the reactants. Although the syntheses have not been carried out in dry conditions, we have experimentally observed that such low RH percentage is sufficient to avoid graphene aggregation.

Films were obtained by dip-coating the substrates into the silica-graphene solution at withdrawal rate of 15 $cm{\cdot}min^{-1}$ and a relative humidity of 25%, the temperature in the deposition chamber was kept at 25°C. After deposition the silica-graphene films were

thermally treated in air at for one hour; the samples were directly put in the oven at the selected temperature (100, 200, 300, 350 and 450°C).

Material characterization.

Raman analysis was done using a Bruker Senterra confocal Raman microscope using a laser excitation of 532 nm and 5 mW of nominal power and a 100 x objective. The spectra were collected in the 70 - 4500 cm^{-1} range, with a resolution of 9 cm^{-1}, an integration time of 3 seconds and 6 coadditions. The number of graphene layer was estimated through Laurentian fit of the Raman spectra in 2820-2560 cm^{-1} range. The fit provided a residual root mean square error RMS < 7.

Fourier transform infrared (FTIR) spectroscopy analysis was performed by a Vertex 70 Bruker spectrophotometer equipped with a RT-DTGS detector and a KBr beam splitter. The spectra were recorded in the 400–4000 cm^{-1} range with a resolution of 4 cm^{-1} using a silicon wafer as the background reference. The baseline was corrected using a concave rubber-band method (OPUS 7.0 software) using 64 baseline points and one iteration.

The film thickness and refractive index were estimated by an α-SE Wollam spectroscopic ellipsometry using an absorbing film model; this technique provided the best fit for a homogeneous coating without refractive index gradient along the thickness. The fit allowed obtaining an average mean square error (MSE) less than 2.

UV-Visible absorption spectra were measured by a Nicolet Evolution 300 spectrophotometer, silica glass was used as background reference.

TEM images were taken using a JEM-2000 FX JEOL instrument operating at 200 kV; fragments obtained by scratching the films were dispersed in ethanol by ultrasonication and then dropped on a carbon-coated copper grid and dried for observations.

Results and Discussion

The deposition of graphene nanocomposite films from a liquid phase through sol-gel processing requires a careful design of the chemistry to obtain optically transparent layers and to avoid aggregation of the graphene sheets. The low solubility of graphene sheets in polar solvents is however limiting the application of sol-gel chemistry for preparing such kind of nanocomposites. A common route to handle with graphene in liquid phase is using its oxidized form, the so-called graphene oxide (GO), which is

obtained by chemical modification of graphite in acidic conditions. GO has a higher solubility with respect to pristine graphene and can be dispersed in polar media; after material preparation the graphene oxide is finally converted into reduced graphene oxide (RGO). Chemical reduction of graphene oxide, however, brings to the formation of an uncontrolled amount of defects in the sheets; furthermore, the application of the process to an oxide nanocomposite is not always a feasible route.

To overtake these limitations we have developed an alternative method that allows using exfoliated graphene (EG) dispersions in sol-gel chemistry. This method produces exfoliated graphene dispersions by ultrasonication of graphite flakes immersed in suitable media.[13, 14] We have used 1-vinyl-2-pyrrolidone (NVP) as a medium, because of its high solubility in ethanol and the capability of dispersing up to several mg of graphene per ml.

The dispersions have been then added to a highly acidic silica precursor sol to obtain a black homogeneous solution; different batches with concentrations ranging from 43.7 up to 700 µl have been used to adjust the amount of graphene in the films.

A key step of the synthesis is employing $SiCl_4$ in anhydrous conditions as precursor instead of a silicon alkoxide, which is commonly used in sol-gel synthesis. In fact, water is necessary for hydrolysis of alkoxides, but its addition causes an immediate precipitation of graphene. Therefore, we have used ethanol as the solvent for $SiCl_4$ and NVP as medium for dispersing graphene; when mixed together, a stable solution is formed.

Addition of ethanol to $SiCl_4$ is the standard route to synthesise tetraethylorthosilicate (TEOS) according to the reaction[15] (1):

$$SiCl_4 + 4\ C_2H_5OH \rightarrow Si\text{-}(OC_2H_5)_4 + 4\ HCl \qquad (1)$$

In anhydrous conditions, condensation of silica is hindered even if formation of SiO_2 based on the elimination of alkyl chloride (RCl) would be in principle possible through the reaction (2):

$$2\ SiCl_4 + 4\ ROH \rightarrow 2\ SiO_2 + 4\ RCl + 4\ HCl \qquad (2)$$

This reaction pathway, however, is observed only with tertiary or benzylic alcohol groups while in the present case we have used a primary alcohol. When $SiCl_4$ is dissolved in an excess of ethanol, it is all transformed in the corresponding silicon alkoxide which does not react in absence of water. At this stage the addition of graphene

dispersion in NVP does not affect the chemistry of the solution. The sol-gel reaction is only triggered during the film deposition when water is absorbed from the external environment; this is why controlling the relative humidity during sol preparation and within the deposition chamber is a critical parameter.

Figure 1 shows the Raman spectra obtained from the EG-silica films treated at 100°C with two different concentrations of graphene; the highest (700 µl) and the lowest one (43.7 µl) of the batch that has been tested. In **Figure 1a** the spectra in the 1700 - 1200 cm^{-1} range are shown; they exhibit three bands: the first one at 1348 cm^{-1}, assigned to breathing mode of κ-point phonons of A_{1g} symmetry (D band); a second one at 1583 cm^{-1}, the first-order scattering of the E_{2g} mode of C sp^2 atoms (G band); a third one at 1620 cm^{-1} (D' band) which is overlapped with the G band and is attributed to Stokes scattering by a longitudinal optical phonon. The spectra in the 3300 - 2500 cm^{-1} interval are reported in **Figure 1b**; also in this range three bands are observed, one at 2706 cm^{-1} (2D band) which is the first overtone of the D band and the sum of two phonons with opposite momentum; another one at 2945 cm^{-1} (D + D' band) due to combination of D and D' bands or G and D bands and a third one at 3246 cm^{-1} (2D' band) assigned to the first overtone of D' band.

The Raman spectra are generally used to obtain an indication about the aggregation state of graphene sheets and the presence of defects[16]. In particular, the D band, which is activated by defects or lattice disorder (non sp^2 composition), indicates the presence of a small amount of lattice disorder in the graphene exfoliated sheets, the higher is the intensity of this band and the larger is the amount of defects[17]. The intensity of the D band does not change with the variation of the different preparation parameters, such as concentration of graphene and thermal annealing (*vide infra*); this indicates that the lattice defects are created by the exfoliation process and not by the processing of the nanocomposite films[18]. On the other hand, the Raman spectra show no significant variations in all the range of concentrations that have been tested (**Figure 1**); the intensity ratio between the 2D and G bands (I_{2D}/I_G ~ 0.5) and the full width at half maximum (FWHM) of the 2D band (~75), which are directly correlated to the number of graphene sheets, do not change with the concentration. This suggests that the EG sheets do not aggregate up to the highest employed concentration.

The number of graphene sheets can be calculated using the 2D band peaking around 2706 cm^{-1}.[19] **Figure 2** shows the Lorentzian fit of the 2D band of the 700 µl graphene sample treated at 100°C; this band, which originates the inter-valley scattering of two in plane transverse optical phonons, provides unambiguous information about the number of constituent graphene layers.[20] In fact, the number of Lorentzian curves that are experimentally required to fit this Raman band depends on the number of graphene sheets aggregated in form of platelets.[21] The best fit of the spectra is obtained using four curves, indicating that in the silica films the sheets are in the form of graphene bilayers. The four components fit is the best one for all the samples and, at least within the 43.7-700 µl range of graphene concentrations, the sheets do not aggregate upon incorporation into the silica matrix.

The structure of the silica host matrix as a function of graphene concentration has been studied by FTIR spectroscopy. **Figure 3a** shows the FTIR absorption spectra in the 1800 - 850 cm^{-1} range of the EG-silica films treated at 100°C. The wide and intense silica Si-O-Si antisymmetric stretching band, ν_{as}(Si-O-Si), peaking at around 1077 cm^{-1} and the Si-OH stretching mode (960 -935 cm^{-1}), are observed.[22] The main silica band is accompanied by a typical intense shoulder at higher wavenumbers (1100–1250 cm^{-1}) which is generally taken as a reference to evaluate the condensation of silica species, especially in the case of sol–gel materials.[23] The spectra of the films at lower graphene concentrations show the typical pattern of silica films; however at concentrations higher of 175 µl the spectra partially overlap with that of NVP, whose relative amount in the sol is increased in accordance to the graphene concentration. The most intense absorption bands attributed to the polymer are peaked at 1670 and 1290 cm^{-1} and have been attributed to C=O stretching of the amide group and C-H bending respectively. The intensity of silica ν_{as}(Si-O-Si) band decreases with the increase of NVP while the shoulder around 1150 cm^{-1} increases; this suggests that the silica condensation is reduced as far as the NVP in the precursor sol increases. The increase in the silica shoulder, which is in part overlapped with NVP bands, indicates a more open and less condensed silica structure. The spectra in **Figure 3b** confirm this indication; the intensity of the OH signal, which is peaking around 3300 cm^{-1}, increases with NVP in the sol; a higher content of OH can be correlated to the presence of uncondensed silanols. The FTIR data show, therefore, that the addition in the precursor sol of NVP,

which is used to separate the graphene sheets, reduces the condensation of the silica matrix; isolated silanols and silanols in small chains are also detected as low intensity bands at higher wavenumbers.[24]At the same time the NVP addition increases the viscosity of the solution and therefore the films thickness increases with the content of NVP, as shown in **Figure 4**. The thickness of the films treated at 100°C and then measured by optical ellipsometry increases from 125 nm (43.7 µl sample) up to 180 nm (700 µl sample); the effect of graphene-NVP dispersion on thickness can be seen comparing the pure silica film with that with 43.7 ml graphene; the addition of graphene-NVP dispersion produces an immediate increase in thickness from 105 to 125 nm. The refractive index also increases as a function of the graphene concentration from 1.38 for undoped film up to 1.55 for 200 µl doped sample.

The optical transparency of the silica-graphene films is an important requirement for development of applications based on the functional properties of graphene such as optical limiting. The UV-Vis absorption spectra of the silica films treated at 100°C with different graphene concentrations are shown in **Figure 5**, they exhibit a high optical transparency up to the UV region with a small absorption band peaking at 239 nm due to π-π* interactions of the aromatic rings.[25] Sol-gel films after deposition are in a soft matter state and must be further processed to remove the residual solvent and obtaining a full densification of the oxide matrix. The graphene-silica films have been therefore thermally treated in air at increasing annealing temperatures to condense the silica structure and remove the NVP from the matrix. **Figure 6 shows t**he Raman spectra of the film, prepared with 700 µl of graphene NVP suspension, after thermal treatment at 100°C and 450°C; the spectra do not reveal significant changes which means that the graphene sheets are stable up to this temperature of annealing. Graphene do not change into the graphene oxide form also because the films are not fluorescent. The oxide matrix acts as a protective system around the graphene sheets and avoid its oxidation, however the thermal process induces a densification of the silica structure. The Raman spectra of the silica graphene films prepared at increasing graphene content and treated at 100°C are also shown in **Figure S1** and **S2** while the Raman spectrum of the pure NVP graphene suspension is reported as a reference in **Figure S3**.

The thermal evolution of the silica-graphene films has been also studied by infrared spectroscopy as a function of the annealing temperature. **Figure 7a and b** show the

spectra of the samples prepared with 700 µl of graphene-NVP dispersion and annealed between 100 and 450°C. Treatments at higher temperatures induce a higher densification of the inorganic matrix, as shown by the increased intensity of the band peaked at 1060 cm^{-1} and the decrease in the absorbed water (broad band between 3800 and 2800 cm^{-1}); at the same time a progressive thermal removal of the NVP is also observed, as shown by the decrease of the band at 1670 cm^{-1}, the triple band in the 1500-1400 cm^{-1} range and the band at 1293 cm^{-1}. Annealing temperatures higher than 200°C removes completely the polymer as also confirmed by the disappearance of bands at 2900 and 2986 cm^{-1}, attributed to the symmetric and anti-symmetric CH_2 stretching.

The thermal stability of the graphene in the oxide matrix has been confirmed by TEM analysis. **Figure 8** shows two representative bright field images of a silica-graphene film prepared with 700 µl of NVP dispersion and treated at 100 and 450°C (a and b). By comparing the TEM images, we can deduce that thermal treatments up to 450°C do not affect the morphology of the graphene aggregates. The graphene sheets, indicated by black arrows in figure, show different morphologies with a lateral size ranging from ≈ 100 nm up to 2-3 µm. The structure of the graphene aggregates is compatible with a 2 or 3-layer graphene formed by sheets with variable dimension; similar structures have been also observed in films prepared at lower graphene concentration.

Conclusions

Graphene sheets in the form of bilayers have been incorporated into a thin silica film via one pot sol-gel process. The synthesis has been designed to avoid graphene precipitation, which is induced by water; $SiCl_4$ in ethanol has been therefore used to dissolve graphene in 1-vinyl-2-pyrrolidone. The silica condensation occurs during film deposition with controlled absorption of water from external environment.

The graphene sheets do not aggregate or degrade upon incorporation in the silica matrix and remain well dispersed; the concentration of graphene can be tuned within a large range without aggregation while the films remain optically transparent. Thermal processing produces the densification of the silica matrix and the full removal of 1-vinyl-2-pyrrolidone without degradation of the films while graphene sheets do not oxidise.

The integration of graphene dispersions in sol-gel solutions without the use of oxidation/reduction chemical pathways, enables a number of functional applications where is required a graphene with a low amount of defects embedded in a stable matrix. The incorporation into optically transparent and durable materials such as silica will allow developing functional coatings to exploit the optical linear and non-linear properties of graphene, such as optical limiters.

References

[1] A. K. Geim, *Science,* 2009, **324**, 1530.

[2] G. K Lim, Z. L. Chen, J. Clark, R. G. S. Goh, W. H. Ng, H. W. Tan, R. H. Friend, P. K. H. Ho and L. L., *Nat. Photonics*, 2011, **5**, 554.

[3] J. Wang, Y. Hernandez, M. Lotya, J. N. Coleman and W. J. Blau, *Adv. Mater.*, 2009, **21**, 2430.

[4] M. Feng, H. B. Zhan and Y. Chen, *Appl. Phys. Lett*., 2010, **96**, 033107.

[5] R. Signorini, M. Meneghetti, R. Bozio, M. Maggini, G. Scorrano, M. Prato, G. Brusatin, P. Innocenzi and M. Guglielmi, *Carbon*, 2000, **38**, 1653.

[6] P Innocenzi, G. Brusatin, M. Guglielmi, R. Signorini, R. Bozio and M. Maggini, J. Non-Cryst. Solids, 2000, **265**, 68.

[7] P. Innocenzi and G. Brusatin, *Chem. Mater*., 2001, **13***,* 3126.

[8] a) S. Stankovich, D. A. Dikin, H. B. Dommett, K.M. Kohlhaas, E. J. Zimney, E. A. Stach, R. D. Piner, S. T. Nguyen and R. S. Ruoff, *Nature*, 2006, **442**, 282. b) S. Bai and X. Shen, *RSC Adv.* 2012, **2**, 64.

[9] L. Malfatti, P. Falcaro, A. Pinna, B. Lasio, M. F. Casula, D. Loche, A. Falqui, B. Marmiroli, H. Amenitsch, R. Sanna, A. Mariani and P. Innocenzi, *ACS Appl. Mater. Interfaces,* 2014, **6**, 795.

[10] Z.-M. Wang, W. Wang, N. Coombs, N. Soheilnia, G. A Ozin ACS Nano, 2010, **4**, 7437.

[11] S. Anandan, T. N. Rao, M. Sathish, D. Rangappa, I. Honma and M. Miyauchi, *ACS Appl. Mater. Interfaces,* 2013, **5**, 207.

[12] L. Han, P. Wang, S. Dong, *Nanoscale* 2012, **4**, 5814.

13 Y. Hernandez, V. Nicolosi, M. Lotya, F. M. Blighe, Z. Sun, S. De, I. T. McGovern, B. Holland, M. Byrne, Y. K. Gun'Ko, J. J. Boland, P. J. Niraj, G. Duesberg, S.

Krishnamurthy, R. Goodhue, J. Hutchison, V. Scardaci, A. C. Ferrari, J. N. Coleman *Nat. Nanotechnol*. 2008, **3**, 563.

[14] D. Nuvoli, L. Valentini, V. Alzari, S. Scognamillo, S. Bittolo Bon, M. Piccinini, J. Illescas, A. Mariani, *J. Mater. Chem*., 2011, **21**, 3428.

[15] A. Vioux, P. H. Mutin, *Handbook of sol–gel science and technology*, ed. S. Sakka, Kluwer Academic Publisher, New York, 2005, vol. 1, ch. 8, pp. 621-639.

[16] M.A. Pimenta, G, Dresselhaus, M.S. Dresselhaus, L.G. Cancado, A. Jorio and R. Saito, *Phys. Chem. Chem. Phys*., 2007, **9**, 1276.

[17] C. Shen, G. Huang, Y. Cheng, R. Cao, F. Ding, U. Schwingenschlögl and Y. Mei, *Nanoscale Res. Lett*., 2012, **7**, 268

[18] M. Quintana, E. Vazquez and M. Prato, *Acc. Chem. Res*., 2013, **46**, 138.

[19] A.C. Ferrari, J. C. Meyer, V. Scardaci, C. Casiraghi, M. Lazzeri, F. Mauri, S. Piscanec, D. Jiang, K. S. Novoselov, S. Roth and A. K. Geim, Phys. Rev. Lett., 2006, 97, 187401.

[20] A. C. Ferrari, *Solid State Commun*. 2007, **143**, 47.

[21] L. M. Malard, M. A. Pimenta, G. Dresselhaus and M. S. Dresselhaus, *Phys. Rep.* 2009, **473**, 51.

[22] P. Innocenzi, *J. Non-Cryst. Solids*, 2003, **316**, 309.

[23] R. M. Almeida, *Phys. Rev. B*, 1992, **45**, 161.

[24] L. Malfatti, T. Kidchob, P. Falcaro, S. Costacurta, M. Piccinini, M. Cestelli Guidi, A. Marcelli, A. Corrias, M. F. Casula, H. Amenitsch and P. Innocenzi, *Microp. Mesoporous Mater.*, 2007, **103**, 113.

[25] G. Eda and M. Chhowalla, *Adv. Mater*., 2010, **22**, 2392.

FIGURE CAPTIONS

Figure 1. Raman spectra in the range 1700 - 1200 cm^{-1} (a) and 3300 - 2500 cm^{-1} (b) of graphene-silica films after thermal treatment at 100°C and prepared from a sol with 43.7 and 700 µl of graphene concentration.

Figure 2. Raman spectra of the 2D band in the 2820-2560 cm^{-1} range measured on graphene-silica films (700 µl of EG dispersion) after thermal treatment at 100°C. The line colours indicate the experimental curve (black line), the global fit (red line) and the single Laurentian fit curves (blue lines).

Figure 3. FTIR absorption spectra in the 1800 - 850 cm^{-1} (a) and 4000 - 2750 cm^{-1} (b) range of graphene-silica samples at different graphene concentrations, the bands assigned to 1-vinyl-2-pyrrolidone are indicated as NVP. The films have been treated at 100°C.

Figure 4. Film thickness (hollow squares) and refractive index (hollow circles) as a function of the graphene concentration in the precursor solution; the films have been treated at 100°C. The lines are guides for eyes.

Figure 5. UV-Vis absorption spectra of the graphene-silica films treated at 100°C at different graphene concentrations. Silica film (black line) is shown as reference.

Figure 6. Raman spectra of the graphene-silica films (700 µl) after thermal treatment at 100 and 450°C.

Figure 7. FTIR absorption spectra in the 1800 - 850 cm^{-1} (a) and 4000 - 2750 cm^{-1} (b) range of graphene-silica samples (700 µl), treated at different temperatures.

Figure 8. Representative bright field TEM images of the silica-graphene nanocomposite films prepared with 700 µl of EG in NVP and treated at 100 (a) and 450°C (b).

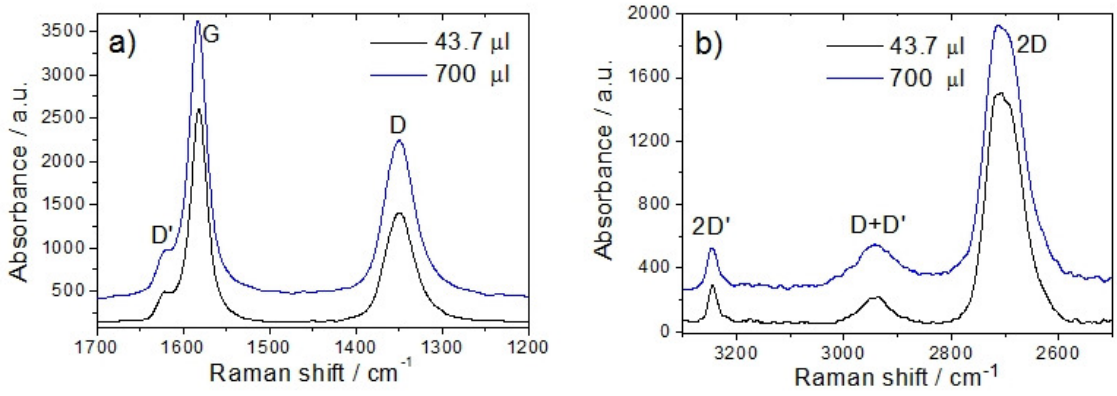

Figure 1

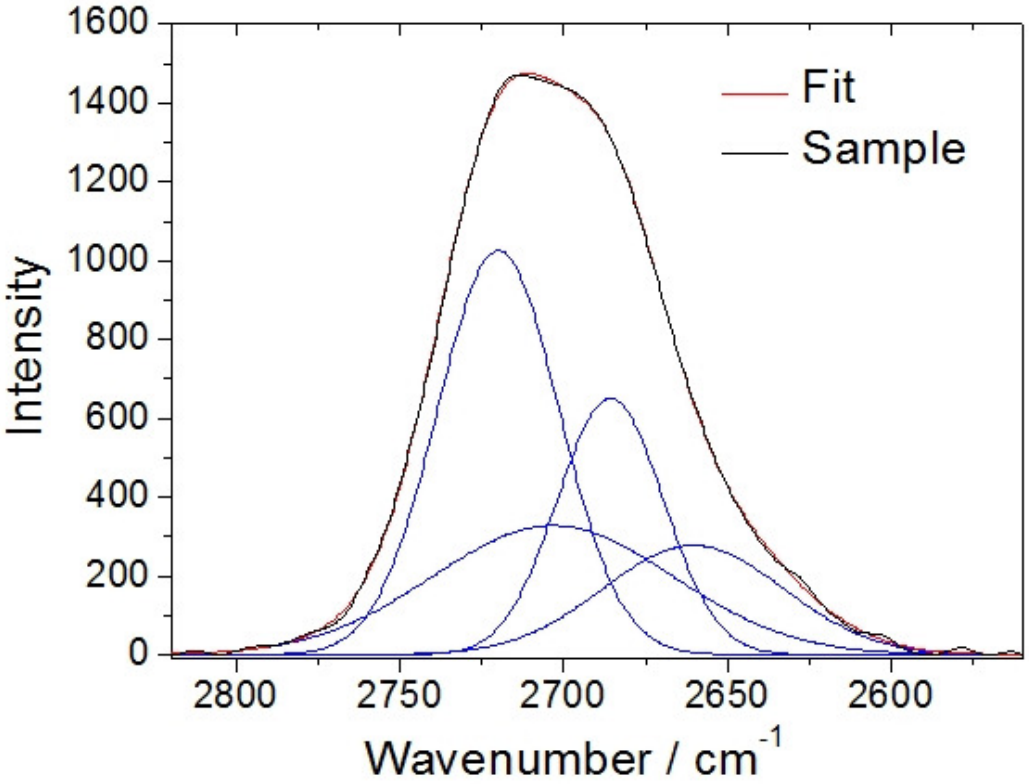

Figure 2

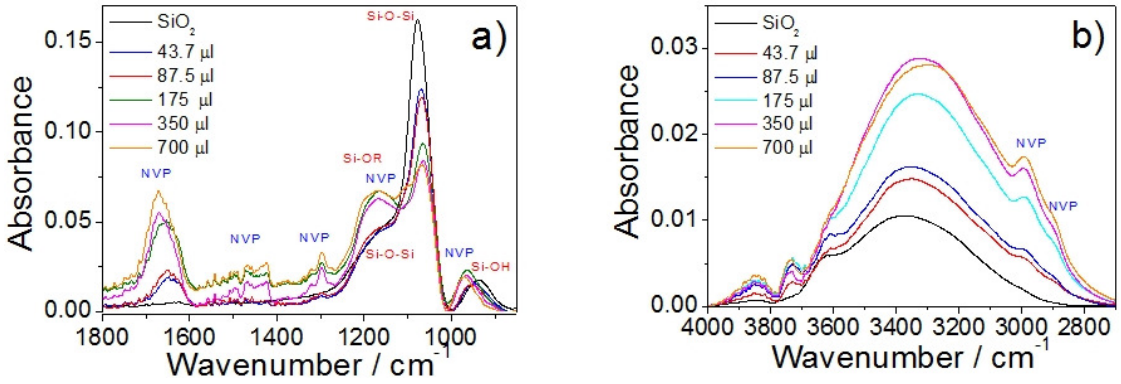

Figure 3

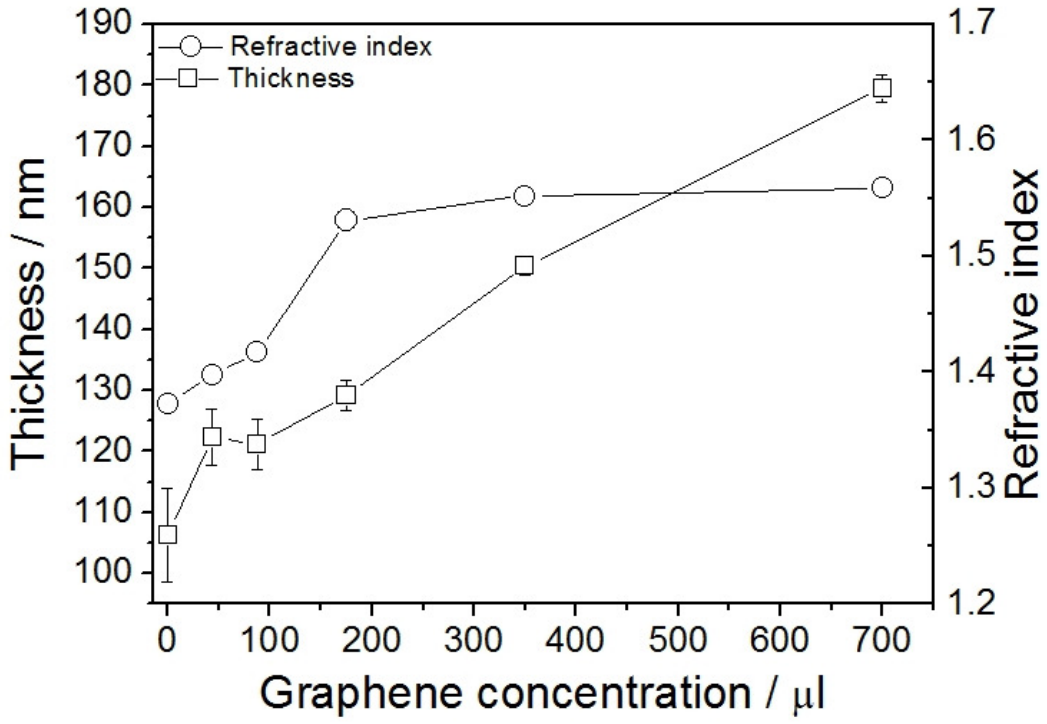

Figure 4

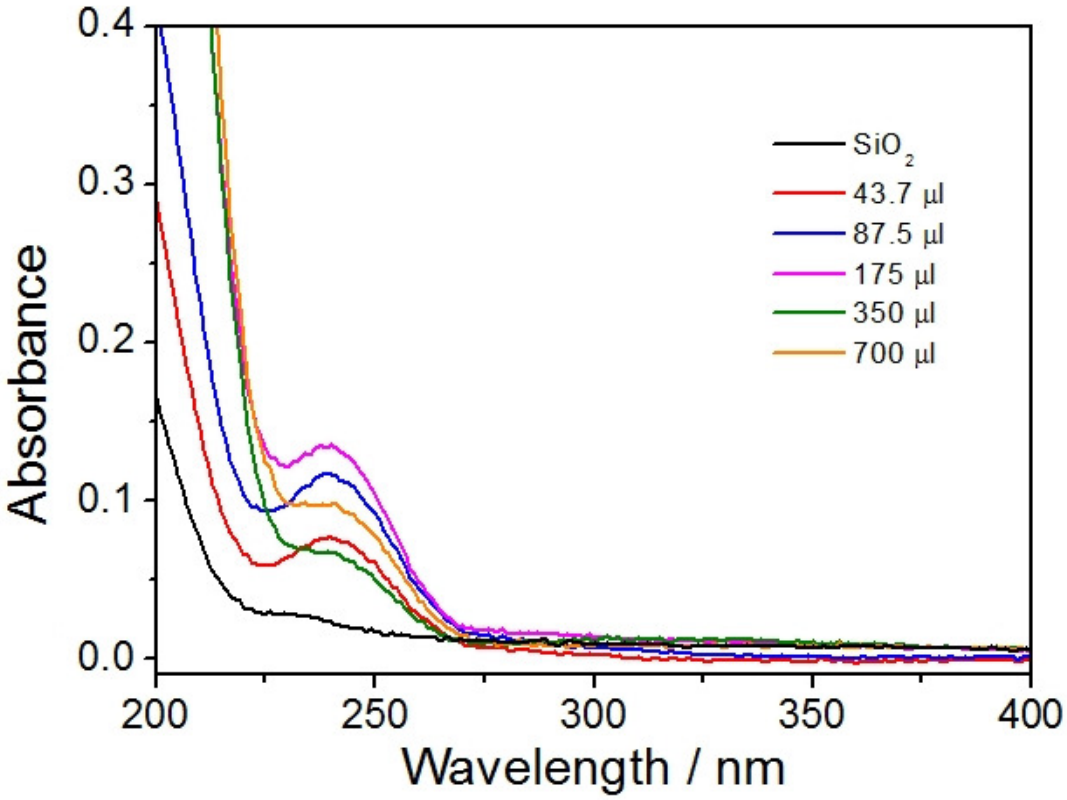

Figure 5

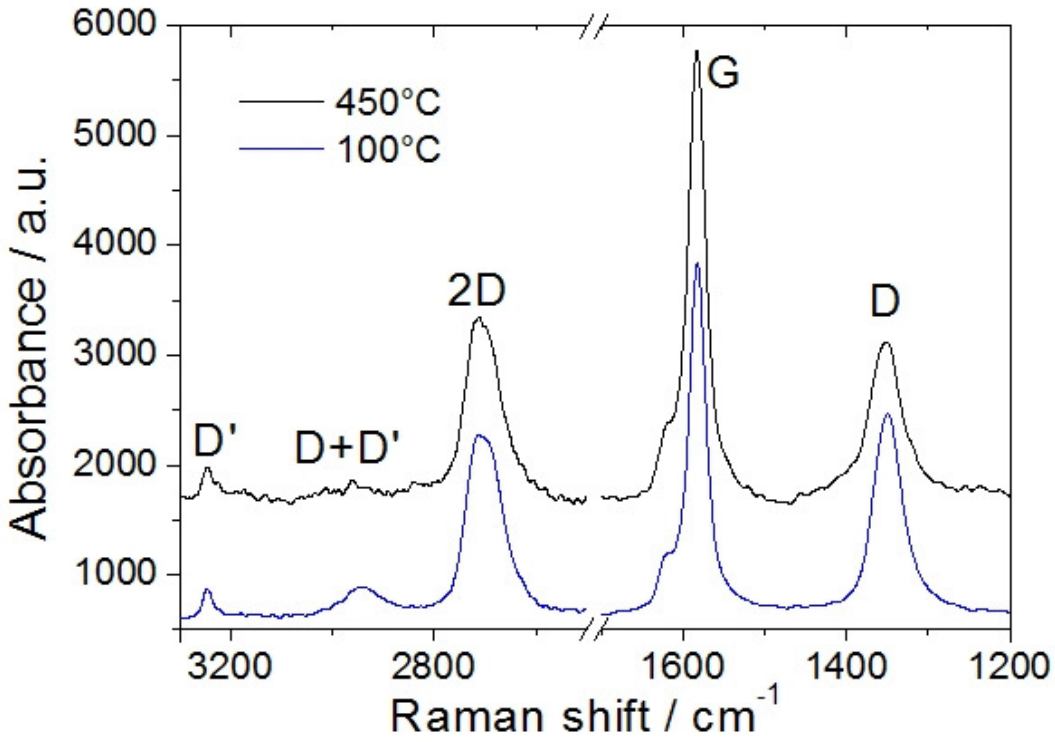

Figure 6

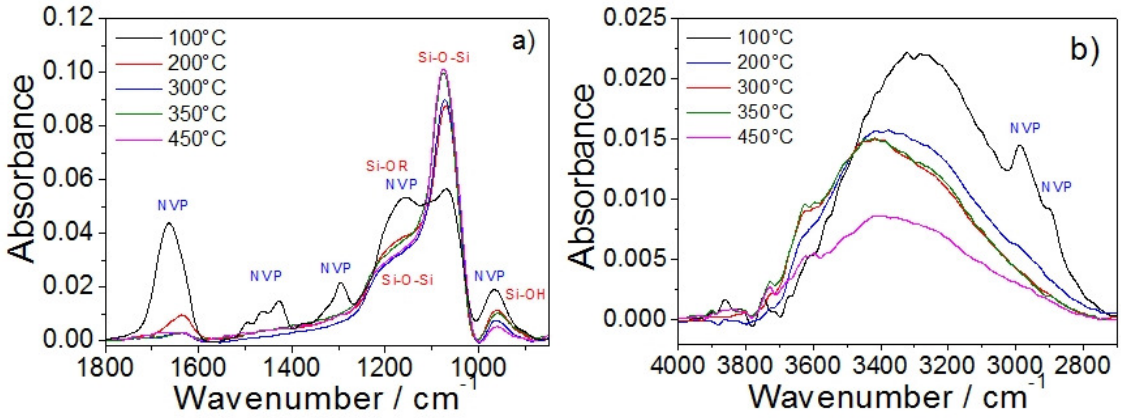

Figure 7

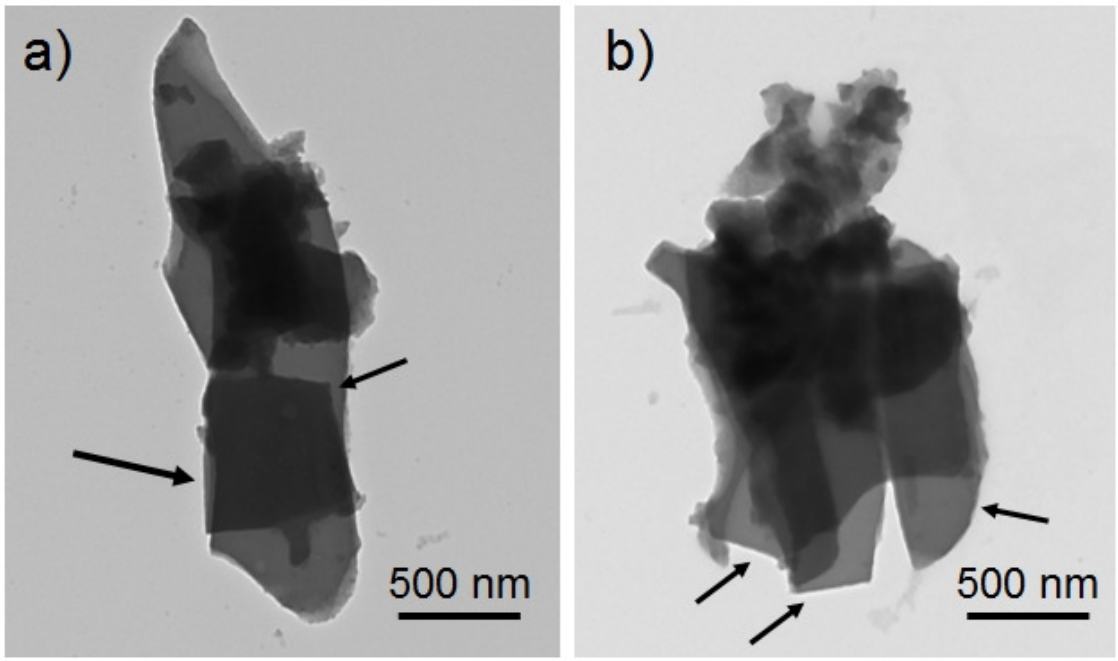

Figure 8